EUROfusion

EUROFUSION WPSA-PR(16) 16757

R Zagorski et al.

Numerical analyses of baseline JT-60SA design concepts with the COREDIV code

Preprint of Paper to be submitted for publication in
Nuclear Fusion

This work has been carried out within the framework of the EUROfusion Consortium and has received funding from the Euratom research and training programme 2014-2018 under grant agreement No 633053. The views and opinions expressed herein do not necessarily reflect those of the European Commission.

Numerical analyses of baseline JT-60SA design concepts with the COREDIV code

R. Zagórski[1], K.Galazka[1], I. Ivanova-Stanik[1], W.Stepniewski[1], L.Garzotti[2], G.Giruzzi[3], R.Neu[4] and M.Romanelli[2]

[1]Institute of Plasma Physics and Laser Microfusion, Hery Street 23, 01-497 Warsaw, Poland
[2]CCFE, Culham Science Centre, Abingdon, Oxon, OX14 3DB, UK
[3]3CEA, IRFM, F-13108 Saint-Paul-lez-Durance, Francey
[4]Max-Planck Institut für Plasmaphysik, 85748 Garching, Germany

Corresponding Author: roman.zagorski@ipplm.pl

Abstract:

JT-60SA reference design scenarios at high (#3) and low (#2) density have been analyzed with the help of the self-consistent COREDIV code. Simulations results for standard carbon wall and the full W have been compared in terms of the influence of impurities, both intrinsic (C, W) and seeded (N, Ar, Ne, Kr) on the radiation losses and plasma parameters. For the scenario #3 in carbon environment the regime of detachment on divertor plates can be achieved with N or Ne seeding, whereas for the low density and high power scenario (#2), the carbon and seeding impurity radiation does not e?ectively reduce power to the targets. In this case only increase of neither average density or edge density together with Kr seeding might help to develop conditions with strong radiation losses and semi-detached conditions in the divertor. The calculations show that in case of tungsten divertor the power load to the plate is mitigated by seeding and the central plasma dilution is smaller compared to the carbon divertor. For the high density case with neon seeding operation in full detachment mode is observed. Ar seems to be an optimal choice for the low density high power scenario #2, showing wide operating window, whereas Ne leads to high plasma dilution at high seeding levels albeit not achieving semi-detached conditions in the divertor.

1 Introduction

JT-60SA is a superconducting tokamak supporting thermonuclear fusion research on the way towards realization of energy production in a DEMO reactor. It will complement ITER in resolving some key engineering and physics issues for DEMO operation[1]. The baseline JT-60SA design foresees full carbon wall, however feasibility studies have been initiated recently to assess the possibility of the transition to full W environment in the extended phase of the JT-60SA operation. According to engineering limits for ITER, the maximum heat dissipated in the divertor plate has to be lower than 10 MW/m^2 in steady state [2]. This can be achieved by radiative cooling in the pedestal and scrape-off

layer (SOL) areas, which helps to spread the energy over a larger area and to reduce the energy flux towards the target and effective radiating cooling can be provided by seeded or intrinsic impurities.

The influence of various seeding gases on the improvement of energy confinement on JT-60U has been already extensively investigated experimentally and numerically. For instance in Ne-seeded discharges neon was found to contribute the dominant part of radiation during detachment [3].

In this paper, JT-60SA reference design scenarios [1] at high (#3) and low (#2) density have been analyzed with the help of the self-consistent core-edge COREDIV code [4]. COREDIV is able to simulate tokamak plasmas with various divertor plate materials as well as various plasma impurities [5, 6, 7, 8, 9]. Simulation results for the standard carbon wall [10] and the planned full tungsten configuration have been compared in terms of the influence of impurities, both intrinsic (C, W) and seeded (N, Ar, Ne, Kr) on the radiation losses and plasma parameters. In particular, the reduction of the divertor target power load due to radiation of sputtered and externally seeded impurities has been investigated.

2 Model Description

The physical model used in the COREDIV code is based on a self-consistent coupling of the 1D transport in the core to the 2D multifluid description of the scrape-off layer and has been already presented elswhere[4, 10, 11]. Although the device geometry and treatment of neutral particles is simplified the code can produce quantitative agreement with experimental observations in a time-efficient manner. The code has been already successfully benchmarked with a number of JET discharges, including the nitrogen seeded type I and type III ELMy H-mode discharges [5, 6, 9] and recently, JET ILW configuration[7]. COREDIV has also been applied to ASDEX discharges in the full W environment[8].

2.1 Core plasma

In the core, the 1D radial transport equations for bulk ions, for each ionization state of impurity ions and for the electron and ion temperature are solved. It is assumed that all ions have the same temperature. For auxiliary heating parabolic-like deposition profile is assumed. The energy losses are determined by bremsstrahlung, synchrotron and line radiation. The equation for the poloidal magnetic field has been neglected and thus the current distribution is assumed to be given in our approach.

The electron and ion energy fluxes are defined by the local transport model proposed in Ref.[12] which reproduces a prescribed energy confinement law. In particular, the anomalous heat conductivity is given by the expression $\chi_{e,i} = C_{e,i}\frac{a^2}{\tau_E}[1 + (\frac{r}{a})^4]F(r)$ where a is the poloidal plasma radius, τ_E is the energy confinement time defined by the ELMy H-mode scaling law (IPB98(y,2))[13] and the coefficient (C_e, C_i ($C_e = 2C_i$) are adjusted to have agreement between calculated and experimental confinement times. The parabolic like profile function is modified to provide transport barrier ($F(r)$) in the plasma edge

with the barrier width of about 5 cm which results in the plasma temperature at the pedestal of the order of 1.2-1.5 keV.

It should be stressed that presented here simplified transport model does not aim on detailed transport predictions for JT-60SA scenarios as done for example in the recent papers of J.Garcia[14] and G.Giruzzi[15]. It is important only that the model reflects the main findings of the more sophisticated transport descriptions like GLF23 or CDBM in terms of the global confinement time and pedestal characteristics. However, benchmarks done with other transport models (JETTO, ASTRA, CRONOS)[16] show that the COREDIV profiles are in reasonable agreement and on top of this it should be stressed that the COREDIV predictions related to the investigations of the impurity influence on the discharge parameters are not very much sensitive to the details of the profiles of the transport coefficients.

The main plasma ion density is given in our approach by the solution of the radial diffusion equation with diffusion coefficients $D_e = D_i = 0.1\chi_e$ and the source term taking into account the attenuation of the neutral density due to ionization processes: $S_i = S_{i0}\exp(-\frac{a-r}{\lambda_{ion}})$, where λ_{ion} is the penetration length of the neutrals, calculated self-consistently. The source intensity S_{i0} is determined by the internal iteration procedure in such a way that the average electron density obtained from neutrality condition equals to that of the scenario considered. The radial impurity transport is described by standard neoclassical model (collisionality dependent) with small contribution from the anomalous transport. The neoclassical impurity transport is based on large aspect ratio assumption and includes both, the diffusion term and the pinch velocity due to density and temperature gradients (off-diagonal terms) corresponding to the contributions from Pfirsch-Schlüter and banana-plateau collisionality regimes. However, for tungsten transport simulations only anomalous contribution gas been considered to avoid W ions accumulation in the core.

2.2 Scrape-off layer plasma

In the SOL we use the 2D boundary layer description[17, 18], which like most other 2D computational plasma edge fluid models is based on the classical transport equations derived by Braginskii [19]. The transport along field lines is assumed to be classical, whereas radial transport is anomalous with prescribed radial transport coefficients. For deuterium ions and for each ionization state of each impurity species we solve the continuity and parallel momentum equations. In addition, two energy equations for electron temperature (T_e) and for one common ion temperature (T_i) are solved. Simplified neutral model is considered in order to avoid time consuming Monte Carlo iterations. It takes into account however, the plasma (deuterium and seeded impurities) recycling in the divertor as well as the sputtering processes at the target plates including deuterium/tritium sputtering, self-sputtering and sputtering due to seeded impurities. We assume that the divertor is in attached (semi-attached) mode and the ratio between electron separatrix density and volume average density is kept constant in our simulations (usually n_{es}=$0.4n_e$). In order to keep the prescribed plasma density at the separatrix (at stagnation point), the deuterium recycling coefficient ($0 < R_H < 1$) is iterated accordingly. The

energy losses due to interactions with hydrogenic atoms and impurities (line radiation, ionization and charge exchange) are accounted for in the model. Although the temperature usually is high at the strike points and, by consequence, physical sputtering is the dominant mechanism for impurity release, also the contribution of chemical sputtering of carbon is considered. The radial transport in the SOL is fixed with radial diffusion $D_{SOL} = 0.5\ m^2/s, \chi_e = 1\ m^2/s,\ \chi_i = 0.5\ m^2/s$.

The standard sheath boundary conditions are imposed at the plates, whereas at the wall the boundary conditions are given by decay lengths. The parallel velocities and the gradients of densities and temperatures are assumed to be zero at the midplane (stagnation point) and at the interface with the private region which is not accounted for in our model. The coupling between the core and the SOL is made by imposing continuity of energy and particle fluxes as well as of particle densities and temperatures at the separatrix. The computed fluxes from the core are used as boundary condition for the SOL plasma, whereas the values of temperatures and of densities calculated in the SOL are used as boundary conditions for the core module. In COREDIV the description of the transport in the core and SOL region is simplified as the main aim is to analyze the influence of the impurities on the radiative heat losses, divertor target load and impurity concentrations. However, one has to take into account the limitations of the model resulting from the assumptions, for instance no implemented treatment of ELM's. Therefore, all the COREDIV results should be interpreted as time-averaged quantities [9].

2.3 Modeled scenarios

In our work we focus on two JT-60SA inductive scenarios: #2 with low density ($n_e = 5.6 \times 10^{19}$ m^{-3}) high heating power ($P_{aux} = 41$ MW) and #3 with high density ($n_e = 9 \times 10^{19}$ m^{-3}) and moderate auxiliary power ($P_{aux} = 30$ MW). Simulations aim at comparison of the standard full carbon (C) configuration with the planned full tungsten (W) environment in terms of the influence of impurities, both intrinsic (C, W) and seeded nitrogen (N), neon (Ne), argon (Ar) and krypton (Kr) on the radiation losses and plasma parameters. In particular, the reduction of the divertor target power load due to radiation of sputtered and externally seeded impurities has been investigated. The main focus is to study the stationary state achieved for different gas seeding levels. As the reference input parameters, we consider $D_{SOL} = 0.5$ m^2/s and n_{es}=$0.4n_e$. However, the influence of changes to these parameters (radial diffusion coefficient in the SOL and electron density at separatrix) on the stationary state is analyzed too. In particular, the total impurity concentrations, radiation losses and corresponding heat loads at the target are calculated. Due to the fact that in #3 the density is higher and the auxiliary power lower than in #2, N or Ne are able to provide enough cooling and therefore simulations with other seeding impurities are omitted.

The main aim of our studies of JT-60SA scenarios[1] was to check whether highly radiating plasmas with strong mitigation of the heat loads can be achieved. The most important tool to realize this goal should be impurity seeding, which is expected to lead to strong edge radiation and mitigation the erosion of target material.

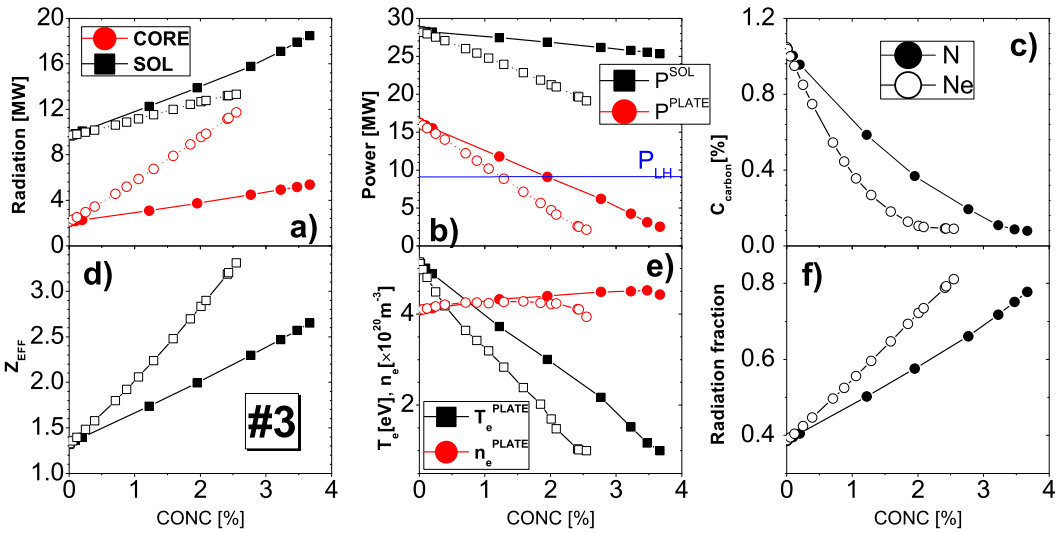

FIG. 1: Main plasma parameters for scenario #3 versus nitrogen (full symbols) and neon (open symbols) concentrations: a) core and SOL radiation; b) power to plate (P^{PLATE}) and to the SOL (P^{SOL}); c) carbon concentration in the core; d) effective charge (Z_{eff}); e) n_e and T_e at the plate (strike point); f) radiation fraction (f_{rad})

2.4 Simulations of JT-60SA scenarios with C wall

For the high density scenario (#3) as well as for low density one (#2), calculations have been performed assuming nitrogen and neon as the reference seeding gases, which appeared to be quite successful in experiments on ASDEX-U and JET with carbon and W walls[8, 6]. However, for low density scenario (#2) seeding by other gasses (Ar, Kr) has been investigated as well. It has been found that all the main plasma parameters of analyzed scenarios can be reasonably reproduced by COREDIV simulations [10].

It should be noted, that for considered scenarios for cases without seeding the power load to target plates is relatively high ($> 16MW$) showing that JT-60SA can work in a power density range relevant for DEMO operation. However, to reduce the heat load to divertor, plasma seeding seems to be necessary for the high power long pulse shots. We point out, that due to the limitations of the model (slab geometry, target perpendicular to the field lines, symmetric divertor) it is impossible to give the correct value of the peak heat flux to the target and therefore in the figures we present only the total power to divertor plates. In the Fig.1, we show the main plasma parameters for the high density scenario #3 versus impurity concentrations for N and Ne seeding. It appears that for this scenario, low Z impurity seeding (N, Ne) leads to the increased plasma radiation ($f_{rad} \sim 80\%$) (Fig.1f) and strong reduction of the power load to the divertor plates. The reduction of P^{PLATE} is mostly due to the increased N_2 or Ne radiation (with increased

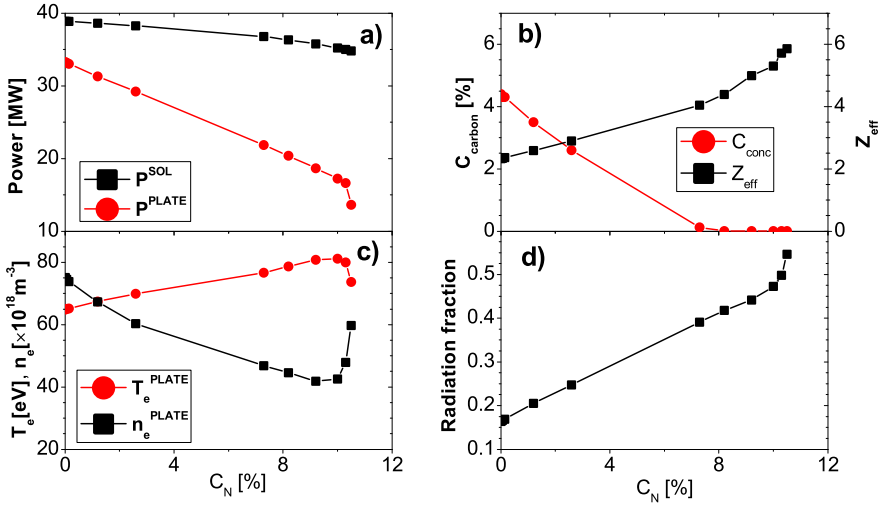

FIG. 2: Main plasma parameters for scenario #2 with C PFCs versus impurity concentrations for N seeding: a) power to plate (P^{PLATE}) and to SOL (P^{SOL}); b) carbon concentration in the core and effective charge (Z_{eff}); c) n_e and T_e at the plate (strike point); d) radiation fraction

puffing), for N mostly in the divertor region whereas for Ne also in the core part of the plasma (Figs.1a and b). For the highest seeding levels, very low plasma temperature in the divertor is achieved ($T_e < 2$ eV)plasma detachment in the divertor can be approached, simultaneously with the reasonable level of the plasma contamination, which however is much higher for Ne. It is achieved thanks to both, efficient screening of impurities by the high density SOL plasma and due to replacement of the carbon ions by nitrogen/neon with carbon erosion almost completely mitigated for highest seeding levels (Fig.1c). The high impurity radiation does not lead however to significant reduction of the power flux through the separatrix ($^{PSOL} > P_{LH}$) allowing for efficient H-mode operation.

In the case of the low density, high power scenario (#2) the situation is different as it can be seen from the Fig.2, where the main plasma parameters are shown versus N_2 concentration. N seeding leads only to a relatively moderate plasma radiation ($f_{rad} \sim$ 60%) and simultaneously large values of the effective charged are seen ($Z_{eff} \sim 6$) leading to strong plasma dilution. In addition divertor conditions are far from plasma detachment with very high plate temperature $T_e > 60$ eV and low plasma density. It should be noted, that even for the highest seeding the power to the target plates might be relatively high ($P_{plate} > 14$ MW).

In order to check how the situation can be improved, simulations with other seeding gasses have been done. We have considered in addition to nitrogen, neon (Ne), argon (Ar) and krypton (Kr) seeding. Some plasma parameters versus Some plasma parameters versus the seeding impurity concentration are shown in the Fig.3. It appears that the situation can not be improved much with other gasses, and radiation fraction higher than 60% can not be achieved. Simultaneously the highest radiation is achieved at high plasma dilution with plate temperatures very high. It has been found that for the low Z seeding gasses (N, Ne) the solution is limited by the plasma dilution, whereas for high Z gases

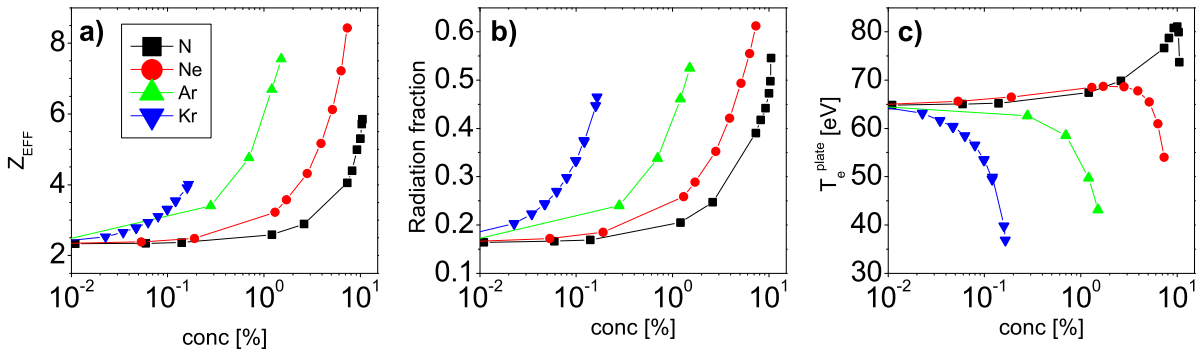

FIG. 3: Main plasma parameters for scenario #2 versus concentrations of seeding gases (N, Ne, Ar and Kr): a) Z_{eff}; b) radiation fraction; c) T_e^{plate} at strike point.

(Ar, Kr) radiative collapse limits the solution. Neon and nitrogen radiate well in edge region but with high Z_{eff}, whereas krypton gives the lowest Z_{eff} and radiates mostly in the core.

However, Kr seeding might be an interesting option for high power shots with somehow higher plasma average or edge density as it can be seen in Fig.4, where comparison for scenario #2 is shown for different average and edge densities: the reference one $n_e = 5.6 \times 10^{19} m^{-3}$, n_{es}=$0.4 n_e$ and higher plasma density ($n_e = 7.5 \times 10^{19} m^{-3}$) or edge density n_{es}=$0.6 n_e$. Highly radiative plasma is clearly achievable for the higher densities, mostly due to the strong krypton radiation in the core leading to overall radiation losses up to 73% (Fig.4a) and reduced power to the plate ($P_{plate} \sim 7 - 8MW$) with reasonable level of plasma contamination ($Z_{eff} \sim 3.5$) and reduced carbon erosion.

Simultaneously the power crossing separatrix remains above the H-L transition threshold ($P_{SOL} > 18MW$). The temperature in the divertor is low (Fig.4b) and the plasma density high, indicating the possibility of the achievement of the semi-detached condition in the divertor region.

3 Results for W divertor

It has been found that in both scenarios with W divertor the power delivered to the divertor plate without seeding is very high and using a seeding gas to control energy exhaust is unavoidable. That conclusion remains valid independent on the assumptions regarding the edge radial transport or edge density values. Calculations done for scenario #3 with Ne seeding and for the reference input parameters (Sec.2.3) show existence of a very wide operating window, since already for relatively low Ne concentrations ($C_{Ne} >$ 0.7%) the divertor heat load is below the technological limit requirements (10 MW/m^2, assuming 1 m^2 of divertor wetting are) whereas the power crossing the separatrix stays above the P_{L-H} power threshold (see Fig.5). The energy losses are dominated by both,Ne and deuterium radiation, and for the maximum applied seeding seeding (C_{Ne} =3.1%) up to 83% of the input power can be radiated with 17.2 MW of Ne radiation and with

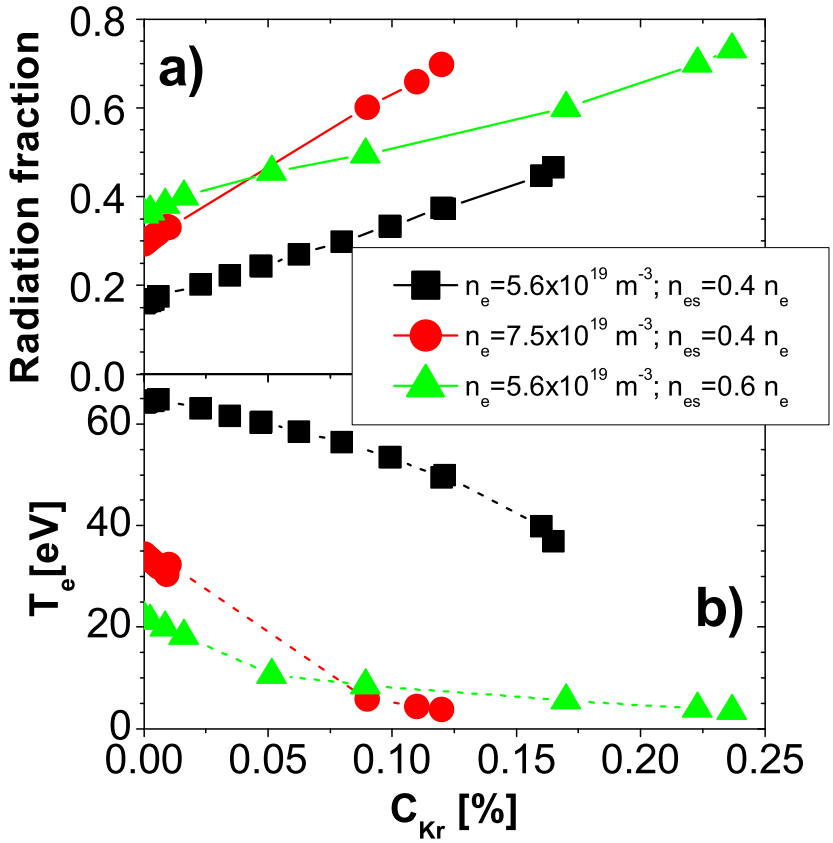

FIG. 4: Main plasma parameters for scenario #2 and for different plasma densities versus Kr concentration: a) radiation fraction; b) T_e at the plate (strike point).

negligible W radiation. Simultaneously the electron temperature at the divertor target is low (∼1 eV) indicating semi-detached conditions (Fig.5).

This rather optimistic result has been further analyzed in terms of different plasma edge parameters (eg. separatrix density, radial anomalous transport). In line with our earlier simulations for JET-ILW [20] and ITER [22] also in the case of JT-60SA it has been found that the increased radial diffusion ($D_{SOL} = 1\ m^2/s$, open symbols in Fig.5) improves the impurity retention in the SOL leading to the increased divertor radiation losses and easier access of detachment. Similar effect on the results has the increased edge density.

In the Fig.6, simulation results are shown for the #2 with tungsten wall and Ne, Ar, and Kr seeding for our reference input parameters (Sec.2.3). It can be seen, that in contrast to the situation with carbon environment, this time seeding by all considered impurities leads to the efficient mitigation of the power flux to the target plates as well as to the reduction of the tungsten production and radiation. Already at reasonable levels of plasma contamination, $C_{Ne} \geq 1.5\%$ ($Z_{eff} \geq 3$), $C_{Ar} \geq 0.3\%$ ($Z_{eff} \geq 2.5$), $C_{Kr} \geq 0.1\%$ ($Z_{eff} \geq 2.6$), the power load to the target is reduced below 10 MW, with the power crossing separatrix above the P_{L-H} threshold. Simultaneously, the plate temperature is low ($T_e^{plate} \leq 7.5eV$, but only fin case of Ar and Kr seeding leads to high plasma density in

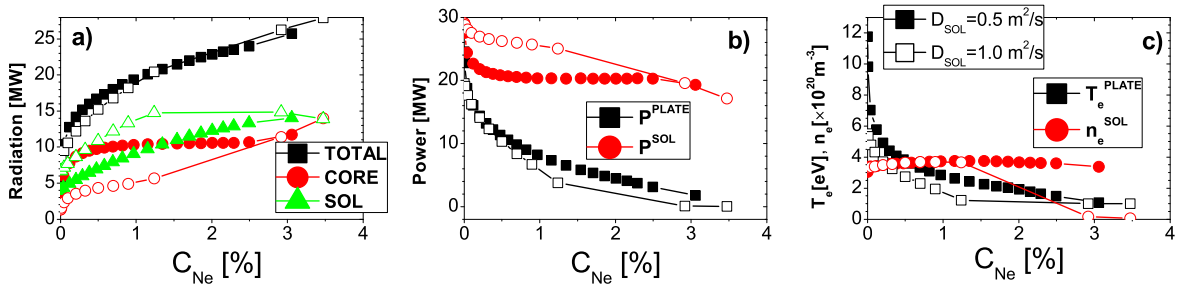

FIG. 5: Main plasma parameters for scenario #3 in W environment versus Ne core concentration: a) total, core and SOL radiations; b) power to divertor targets (P^{PLATE}) and to the SOL (P^{SOL}); c) electron density (n_e) and temperature (T_e) at the target (strike point)

the divertor, whereas for Ne the strong plasma dilution at highest seeding levels prevents the achievement of the high deuterium densities in divertor regions. Therefore, medium Z impurities (Ar, Kr) seems to be optimal seeding gasses for the low density, high power operation of the JT-60SA tokamak with tungsten walls. The operating window, in terms of the range of the seeding gas influx, is the largest for Ar seeding. Moreover, with Argon seeding operations in the less optimistic situation with reduced plasma transport in the SOL ($D_{SOL} = 0.25\ m^2/s$) is also possible. It should be noted that in the case of Ne and Ar seeding, the core W radiation is always the dominant radiation loss channel, whereas krypton can replace energy losses associated with W ions in the plasma core.

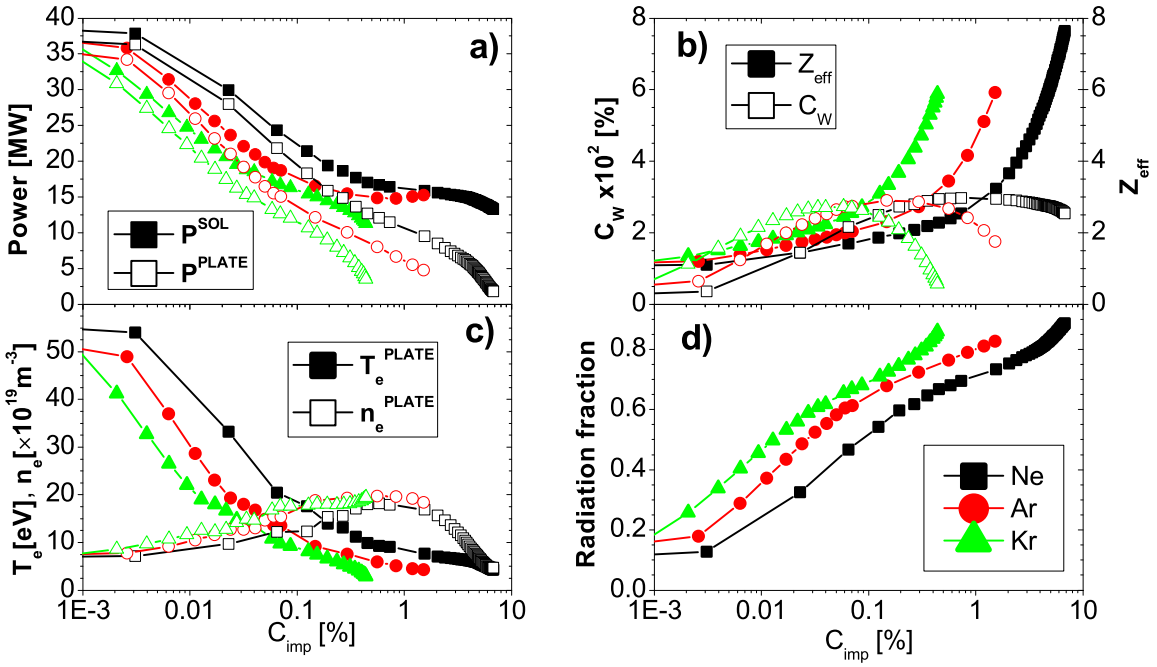

FIG. 6: Plasma parameters for scenario #2 in W environment versus Ne, Ar and Kr concentrations: a) power to divertor targets (P^{PLATE}) and to the SOL (P^{SOL}); c) electron density and temperature at the target (strike point); d) radiation fraction.

4 Conclusions

The reduction of divertor target power load due to radiation of sputtered and externally seeded impurities was investigated by means of numerical simulations of JT-60SA discharges with the COREDIV code. Calculations were performed for JT-60SA scenarios with carbon walls assuming seeding of different gasses (N, Ne, Ar, Kr).

Carbon wall

For all scenarios considered N and C radiates predominantly in the SOL region, Ne starts to radiate also in the core, whereas Ar and Kr radiate mostly in the bulk plasma. For all scenarios with nitrogen (or Ne) seeding, gradual replacement of carbon by low Z seeding impurity is observed as the gas influx increases. For the high density scenario #3 the regime of detachment on divertor plates can be achieved with N and Ne seeding. For high auxiliary power and low density scenarios, the carbon and seeding impurity radiation does not effectively reduce power to plate and consequently, results with very high Z_{eff} (about 6-8) and impurity concentrations ($> 9\%$) are observed. The use of impurity seeding with higher atomic number does not help much but krypton might be very useful in particular when the plasma density is increased. In the case of low density scenarios, increase of neither average density or edge density together with Kr seeding might lead to the development of very favorable conditions in the discharge with strong radiation losses and semi-detached conditions in the divertor.

Tungsten wall

It has been found that in both scenarios with W divertor the power delivered to the divertor plate without seeding is very high and using a seeding gas to control energy exhaust is necessary. For the scenario #3 with Ne seeding and for the reference input parameters a wide operating window, has been found, since already for relatively low Ne concentrations ($C_{Ne} \geq 0.7\%$) the divertor heat load is below the technological limit requirements (10 MW/m^2) whereas the power crossing the separatrix stays above the P_{L-H} power threshold. The energy losses are dominated by Ne and deuterium radiation and for maximum applied seeding up to 83% of the input power can be radiated and semi-detached divertor operation is observed.

In the case of the scenario #2, seeding by nobel gasses (Ne, Ar, Kr) leads to efficient plasma cooling and tolerable heat loads to the target plates ($< 10MW$) at reasonable contamination level ($Z_{eff} \sim 3$). Argon seems to be optimal choice for this low density high power scenario, showing the widest operating window, Ne leads to high plasma dilution at high seeding levels preventing the achievement of semi-detached conditions in the divertor. However, using krypton as a seeding gas has an advantage that it replaces tungsten in the central plasma and limits its concentration.

Simulations results for tungsten environment indicate that it might be reasonable to consider in the case of carbon wall seeding scenario with the mixture of two seeding gasses: high Z gas like Xe which would play similar role to tungsten and radiate in the core and medium Z gas (e.g Ar) to radiate the power in the edge region. Such simulation are planned for the close future.

Acknowledgement: This work has been carried out within the framework of the EUROfu-

sion Consortium and has received funding from the Euratom research and training programme 2014-2018 under grant agreement No 633053. The views and opinions expressed herein do not necessarily reflect those of the European Commission. This scientific work was financed within the Polish framework of the scientific financial resources in 2015-2016 allocated for realization of the international co-financed project.

References

[1] JT-60SA Research Plan - Research Objectives and Strategy Version 3.2 2015, February,*www.jt60sa.org/pdfs/JT-60SA Res Plan.pdf*

[2] ITER Physics Expert Group on Divertor, ITER Physics Expert Group on Divertor Modelling, and Database and ITER Physics Basis Editors. Chapter 4: Power and particle control. Nucl. Fusion, **39** (12):2391 (1999)

[3] NAKANO, T., et. al.,. Contribution of Ne ions to radiation enhancement in JT-60U divertor plasmas. J. Nucl.Materials, **438**, Supplement:S291-S296 (2013)

[4] ZAGÓRSKI, R., et al., Nucl. Fusion **53** (2013) 073030

[5] ZAGÓRSKI, R. et al., J. Nucl. Materials, **390-391** (2009) 404

[6] RAPP, J., et al., J. Nuclear Materials, **337-339** (2005) 826

[7] TELESCA, G. et al, J. Nucl. Materials **438**, Supplement, July 2013, S567

[8] ZAGÓRSKI, R., et al., Contrib. Plasma Phys. **52** (2012) 379

[9] TELESCA, G., et al., Plasma Phys. Control. Fusion **(53)**, 115002 (2011)

[10] ZAGÓRSKI, R., et al Nucl. Fusion **56** (2016) 016018

[11] ZAGÓRSKI, R. et al., Contrib. to Plasma Phys.,**48**, No. 1-3 (2008) 179

[12] MANDREKAS, J., and STACEY, W.M., , Nucl. Fusion **35** (1995) 843

[13] ITER Physics Guidelines, ITER report **N 19. FDR 1 01-07-13 R 0.1**

[14] GARCIA, J., et al., Nucl. Fusion **54** (2014) 093010

[15] GIRUZZI, G., et al., 2012 Model validation and integrated modelling simulations for the JT-60SA tokamak, 24th IAEA Fusion Energy Conf. (San Diego, USA, 2012) **TH/P2-03**, *http://www-naweb.iaea.org/napc/physics/FEC/FEC2012/papers/34_THP203.pdf*

[16] K.Galazka, private communication, WPSA Modelling Meeting, Warsaw, October, 2015

[17] LEIGHEB, M., et al., J. Nucl. Mater. **241-243** (1997) 914

[18] GERHAUSER, H., et al., Nucl. Fusion **42** (2002) 805

[19] BRAGINSKII, S.I., , Rev. Plasma Phys. **1** (1965) 205

[20] ZAGÓRSKI, R. et al., J. Nucl. Materials, **463** (2015) 649

[21] IVANOVA-STANIK, I., et al., J. Nucl. Materials, **463** (2015) 596

[22] ZAGÓRSKI, R. et al., Nucl. Fusion **55** (2015) 053032